Food and Chemical Toxicology 127 (2019) 89–100

Contents lists available at ScienceDirect

Food and Chemical Toxicology

journal homepage: www.elsevier.com/locate/foodchemtox

Shape-engineered titanium dioxide nanoparticles (TiO_2-NPs): cytotoxicity and genotoxicity in bronchial epithelial cells

Marta Gea[a], Sara Bonetta[a,*], Luca Iannarelli[b], Andrea Mario Giovannozzi[b], Valter Maurino[c], Silvia Bonetta[a], Vasile-Dan Hodoroaba[d], Caterina Armato[a,e], Andrea Mario Rossi[b], Tiziana Schilirò[a]

[a] Department of Public Health and Pediatrics, University of Turin, Piazza Polonia 94, 10126, Turin, Italy
[b] Quality of Life Division, National Institute of Metrological Research, Strada delle Cacce 91, 10135, Turin, Italy
[c] Department of Chemistry, University of Turin, Via Giuria 7, 10125, Turin, Italy
[d] Surface Analysis and Interfacial Chemistry division, Federal Institute for Materials Research & Testing (BAM), 12200, Berlin, Germany
[e] Centre for Sustainable Future Technologies (CSFT@PoliTo), Italian Institute of Technology, Corso Trento 21, 10129, Turin, Italy

ARTICLE INFO

Keywords:
Shape-engineered TiO_2 nanoparticles
Genotoxic and oxidative damage
Comet assay
Cytotoxicity
Raman spectroscopy

ABSTRACT

The aim of this study was to evaluate cytotoxicity (WST-1 assay), LDH release (LDH assay) and genotoxicity (Comet assay) of three engineered TiO_2-NPs with different shapes (bipyramids, rods, platelets) in comparison with two commercial TiO_2-NPs (P25, food grade). After NPs characterization (SEM/T-SEM and DLS), biological effects of NPs were assessed on BEAS-2B cells in presence/absence of light. The cellular uptake of NPs was analyzed using Raman spectroscopy.

The cytotoxic effects were mostly slight. After light exposure, the largest cytotoxicity (WST-1 assay) was observed for rods; P25, bipyramids and platelets showed a similar effect; no effect was induced by food grade. No LDH release was detected, confirming the low effect on plasma membrane. Food grade and platelets induced direct genotoxicity while P25, food grade and platelets caused oxidative DNA damage. No genotoxic or oxidative damage was induced by bipyramids and rods. Biological effects were overall lower in darkness than after light exposure. Considering that only food grade, P25 and platelets (more agglomerated) were internalized by cells, the uptake resulted correlated with genotoxicity.

In conclusion, cytotoxicity of NPs was low and affected by shape and light exposure, while genotoxicity was influenced by cellular-uptake and aggregation tendency.

1. Introduction

Nanoparticles (NPs) are defined as particles having their three dimension in the range of 1–100 nm (ISO, 2015). Actually, many consumer products incorporates NPs. The technological, medical and economic benefits of NPs are considerable, but the presence of nanoparticles in the environment could cause adverse effects to humans. NPs have a greater surface area per mass unit, so they potentially have an increased biological activity compared to fine particles. Moreover, NPs size is comparable to the size of cellular structures, so NPs might potentially emulate biological molecules or interfere physically with biological processes (Magdolenova et al., 2012a).

TiO_2 is the oxide of titanium and it has different crystalline structures: anatase, brookite and rutile. Brookite is not produced by industry and is not incorporated in commercial products. In contrast, rutile and anatase are largely used in commercial products (Jovanovic, 2015). TiO_2 is one of the most frequently applied NPs and it is in the top five NPs used in consumer products (Shi et al., 2013). TiO_2-NPs produced are used primarily as a pigment owing to their brightness, resistance to discoloration and high refractive index. As a pigment, TiO_2-NPs are incorporated in paints, plastic materials, paper, foods, medical products and cosmetics. Due to its catalytic and photocatalytic properties, TiO_2 is also used as an antimicrobial agent and a catalyst for purification of air and water (Bonetta et al., 2013; Tomankova et al., 2015).

TiO_2-NPs could be engineered in terms of shapes and sizes by changing synthesis conditions such as raw material, temperature, acidic and alkaline conditions. Engineered TiO_2-NPs with various shapes (e.g. rods, dots and belts) have been prepared for different applications (Bernard and Curtiss, 2005; Sha et al., 2015; Wang et al., 2004). In particular, engineered fiber-shaped nanomaterials (i.e. nanowires,

* Corresponding author. Department of Public Health and Pediatrics, University of Torino, Piazza Polonia 94, 10126, Turin, Italy.
E-mail address: sara.bonetta@unito.it (S. Bonetta).

https://doi.org/10.1016/j.fct.2019.02.043
Received 30 November 2018; Received in revised form 14 February 2019; Accepted 27 February 2019
Available online 05 March 2019
0278-6915/

List of abbreviations

BEAS-2B	Human bronchial epithelial cells
D_h	Hydrodynamic diameter
Fpg	Formamidopyrimidine glycosylase
NP	Nanoparticle
TiO_2	Titanium dioxide

nanotubes) are very attractive because they showed higher activity and advantages in photocatalysis, charge transfer and sensing applications due to their structure (Hamilton et al., 2009). However, these new and enhanced properties may also induce higher toxicological effects upon exposure with biological tissues.

Humans can be exposed to TiO_2-NPs via three portals of entry: oral (mainly via food consumption), dermal (often through cosmetic and sunscreen applications) and inhalation (mainly under occupational and manufacturing conditions) (Warheit and Donner, 2015).

Based on the evidence that TiO_2 can induce lung cancer in rats, TiO_2-NPs were classified as possibly carcinogenic to humans (group 2B) by the International Agency for Research on Cancer (IARC, 2010). Indeed, the inhalation and instillation of rutile and anatase TiO_2-NPs induced lung tumors (Xu et al., 2010), broncho-alveolar adenomas and cystic keratinizing squamous cell carcinomas (De Matteis et al., 2016; Mohra et al., 2006). TiO_2-NPs were also classified as potential occupational carcinogens by the National Institute for Occupational Safety and Health (NIOSH, 2011; Chen et al., 2014).

Many *in vitro* studies showed cytotoxicity, genotoxicity and oxidative effects induced by TiO_2-NPs through oxidants generation, inflammation and apoptosis (Jugan et al., 2011; Karlsson et al., 2015; Park et al., 2008; Shi et al., 2010). The potential of NPs to cause DNA damage is an important aspect that needs attention due to possible mutations and carcinogenesis. Physico-chemical characteristics of NPs have an important role in toxicity. Different studies showed that biological effects can be influenced by crystalline structure, size, shape, exterior area, agglomeration/aggregation and surface properties (Bhattacharya et al., 2009; Johnston et al., 2009). Some studies revealed that crystalline structure probably influences the induced toxicity, in particular the anatase seems to be more reactive (Sayes et al., 2006) and induces more toxic, genotoxic and inflammatory effects, than the rutile (Falck et al., 2009; Petkovic et al., 2011; Xue et al., 2010). However, other studies gave contradictory results with rutile forms being more toxic than anatase (Gurr et al., 2005; Numano et al., 2014; Uboldi et al., 2016). The effect of agglomeration/aggregation of NPs on toxicity is not well understood yet. In recent studies, some authors demonstrated that agglomeration can influence NPs genotoxicity (Magdolenova et al., 2012b; Prasad et al., 2013).

Although physico-chemical properties of NPs can have an important role in the impact on their toxicity, only few studies on shape dependent TiO_2 toxicity has been conducted (Allegri et al., 2016; Hamilton et al., 2009; Park et al., 2013). Additional studies are needed to evaluate the role of shape on TiO_2-NPs toxicity in order to produce useful data for assessing the safety of engineered NPs.

To address this issue, the aim of this study was to investigate cytotoxicity (WST-1 assay), LDH release (LDH assay) and genotoxicity (Comet assay) of three types of engineered TiO_2-NPs of different shapes (bipyramids, rods and platelet NPs) in BEAS-2B (cells isolated from human bronchial epithelium) in comparison with two commercial types of TiO_2-NPs (P25 and food grade). Since the exposure to TiO_2-NPs mainly occurs through respiratory tract (occupational and manufacturing conditions), human cells of the respiratory system (such as BEAS-2B), were selected as a good cell model for *in vitro* toxicology tests. All the TiO_2-NPs in this study were first physico-chemically characterized, even in different culture media to study their agglomeration state, and then they were biologically evaluated. In order to take into account the photocatalytic properties of the TiO_2-NPs, we investigated the cytotoxicity and genotoxicity on BEAS-2B under light exposure and in darkness. Moreover, a modern application of Raman spectroscopy, the 3D confocal Raman imaging, was used to study the uptake of the NPs within the BEAS-2B cells, as the Raman spectra provide information about both organic molecules and solid NPs simultaneously (Ahlinder et al., 2013).

2. Materials and methods

2.1. Synthesis and preparation of TiO_2 NPs dispersion

Rods and bipyramids TiO_2-NPs were synthesized by the forced hydrolysis of an aqueous solution of Ti^{IV}(triethanolamine)$_2$titanatrane (Ti(TEOAH)$_2$), using triethanolamine (TEOA) as shape controller; pH of synthesis was adjusted by adding 1 M NaOH solution; details of these procedures were previously reported (Iannarelli et al., 2016; Lavric et al., 2017). The synthesis of platelet NPs was performed with a solvothermal method (Han et al., 2009; Zhang et al., 2012). In a typical synthesis: a precise volume of $Ti(OBu)_4$ was added in a 150 ml Teflon pot and the desired volume of concentrated hydrofluoric acid was added dropwise under stirring. The Teflon pot was sealed and kept under stirring at high temperature (250 °C) for 24 h in autoclave. The resulting paste was centrifuged three times and washed with acetone and with water (Milli-Q) to remove the residual organics. The synthesis dispersions were subjected to dialysis process (against ultrapure water, using Spectra/Por dialysis membrane tubing MWCO 8–14 kDa) in order to clean the medium. To avoid agglomeration and precipitation, dimethylsulfoxide (DMSO 1% in water) was added to the NPs dispersions (final concentration 2.5 mg/ml); the dispersions were homogenized using an ultra-sonication procedure (Iannarelli et al., 2016), few hours before the exposure with cells.

The same procedure was employed in the preparation of the dispersion of commercial TiO_2 powders, which were the P25 NPs (Evonik), extensively used in toxicity studies (Karlsson et al., 2015; Magdolenova et al., 2014; Valant et al., 2012), and the food grade NPs (Faravelli Group), incorporated in many edible products (Weir et al., 2012).

2.2. Scanning electron microscopy (SEM) including transmission mode (T-SEM)

The dimensional characterization (size and shape) of TiO_2-NPs was carried out with SEM using a Zeiss Supra 40 instrument (Zeiss) equipped with a Schottky field emitter, the standard secondary electrons, i.e. Everhart-Thornley, detector and a high-resolution In-lens detector. The surface-sensitive In-lens SEM mode better suited to morphological/shape analysis and transmission mode in SEM (T-SEM) better suited for dimensional measurements were applied complementary to the same field of view on the sample.

2.3. Dynamic Light Scattering (DLS) analysis

Delsa Nano™ C Analyzer (Beckman Coulter) equipped with a 638 nm diode laser and a temperature control was used for the DLS measurements. The laser fluctuation was detected on a photomultiplier tube detector positioned behind the cuvette with an angle of 163°. Hydrodynamic diameters were calculated setting temperature at 25 °C, viscosity (η) 0.890 cP and refractive index of water 1.3325. In order to simulate the culture medium conditions, DLS analyses were conducted on dilution of TiO_2 dispersions (1:4) in a 1% DMSO aqueous solution, as reference analysis, and in base RPMI 1640 medium [supplemented with l-glutamine (4 mM) and penicillin-streptomycin (100 U/ml - 100 µg/ml)] and complete RPMI 1640 medium [supplemented with FBS (10% v/v), l-glutamine (4 mM) and penicillin-streptomycin (100 U/ml - 100 µg/ml)].

2.4. Raman spectroscopy analysis

The aqueous suspensions of the TiO_2-NPs under investigation were freeze-dried to obtain a solid powder. Raman spectroscopy was used in the analysis of dry TiO_2-NPs powder using a DXR™ Raman Microscope (Thermo Scientific) with a laser wavelength at 532 nm, a laser power of 1 mW and a 10× microscope objective. Spectra were collected in the 50–1800 cm^{-1} spectral region, with a grating resolution of 3.3–3.9 cm^{-1}, exposure time of 1 s and 20 scans in total.

2.5. Cell culture and exposure

BEAS-2B cells, isolated from human bronchial epithelium, were obtained from the American Type Culture Collection (ATCC® CRL-9609™). BEAS-2B were grown as a monolayer, maintained and treated in complete RPMI 1640 medium [supplemented with FBS (10% v/v), l-glutamine (4 mM) and penicillin-streptomycin (100 U/ml - 100 µg/ml)], at 37 °C in a humidified atmosphere containing 5% CO_2.

The solution of NPs (2.5 mg/ml, DMSO 1% in water) was vortexed and sonicated (30 min) in order to homogenize the NPs. NPs (5–160 µg/ml) were directly pipetted in culture plates containing RPMI 1640 medium; then the cell culture plates were mixed on a shaker (10 min). The cells were exposed for 1 h under laboratory light and then they were incubated at 37 °C in darkness (23 h) (exposure with light). In order to standardize the exposure with light the cells were exposed in a dark room (obscured by daylight) to a normal laboratory lamp (36 W/840 Lumilux Cool White-36 W, 3350 lm, 4000 K, supplied from OSRAM lighting AG). The lamp illuminance measured with Quantum photo/radiometer HD 9021 (Delta Ohm) was 289 ± 11 lx. To quantify effects due to the photocatalytic activity of TiO_2, cells were exposed for 24 h in darkness (exposure in darkness).

After exposure, cytotoxicity and genotoxicity assays were performed.

2.6. Cytotoxicity

Cell viability was assessed using Cell Proliferation Reagent WST-1 (Roche). The assay was performed as previously descripted by Gea et al. (2018). Briefly, BEAS-2B cells were cultured in 75 cm^2 flasks and maintained until the cells reached 70% confluence; cells were then seeded in 24-well plates (5×10^4 cells/well) and allowed to adhere overnight. After that, culture medium was removed and cells were exposed to NPs (5, 10, 20, 50 and 80 µg/ml, equivalent to 1.3, 2.6, 5.2, 13.0 and 20.7 µg/cm^2) for 24 h with light or in darkness (as specified in paragraph 2.5). After exposure, WST-1 was added (50 µl/well) and incubated for 3 h (37 °C). After incubation, well contents were centrifuged and the supernatants were transferred in 96-well plate to remove the interference owing to the NPs. The absorbance was measured at 440 nm (Tecan Infinite Reader M200 Pro). Absorbance of unexposed cells was used as negative control. Data were expressed as a percentage of viability. All experiments were performed in quadruplicate (four wells for each experimental condition).

As indicator of cell membrane damage, lactate dehydrogenase activity was measured in cell-free culture supernatants using the LDH assay kit (Cytotoxicity Detection Kit PLUS, Roche) modified for NPs exposure. Briefly, BEAS-2B cells were cultured in 75 cm^2 flasks and maintained until the cells reached 70% confluence, cells were then seeded in 24-well plates (5×10^4 cells/well) and allowed to adhere overnight. After that, culture medium was removed and the cells were exposed to NPs (5, 10, 20, 50 and 80 µg/ml, equivalent to 1.3, 2.6, 5.2, 13.0 and 20.7 µg/cm^2) for 24 h with light or in darkness (as specified in paragraph 2.5). After exposure, the contents of each well were centrifuged to remove the interference owing to the NPs. Each supernatant (100 µl) was transferred into 96-well plate, mixed with Reaction Mixture (100 µl/well) and incubated for 30 min at 15–25 °C. After incubation, Stop Solution (50 µl/well) was added and the absorbance was measured at 490 nm (Tecan Infinite Reader M200 Pro). Absorbance measurement of unexposed cells were used as negative control, while absorbance measurement of unexposed cells lysed with Lysis Solution (Cytotoxicity Detection Kit PLUS, Roche) was used as positive control. Data were expressed as a percentage of LDH release, respect to control cells (100%). All experiments were performed in triplicate (three wells for each experimental condition).

2.7. Genotoxicity

The alkaline Comet assay was used for DNA damage evaluation (direct DNA damage). BEAS-2B cells were cultured in 75 cm^2 flasks and maintained until the cells reached 70% confluence; cells were then seeded in 6-well plates (3×10^5 cells/well) and cultured overnight before exposure to NPs. The cells were exposed to different doses of NPs (20, 50, 80, 120 and 160 µg/ml, equivalent to 5.2, 13.0, 20.7, 31.2 and 41.6 µg/cm^2) for 24 h with light or in darkness (as specified in paragraph 2.5). Unexposed cells and cells treated with DMSO (1%) were used as negative controls. The alkaline Comet assay was performed according to Tice et al. (2000) after slight modifications (Bonetta et al., 2019). After exposure, cells were washed with base RPMI 1640 and PBS, detached using trypsin-EDTA (1×) and cell viability was determined (trypan blue staining). Cells were then centrifuged and mixed with low melting point agarose (0.7%), placed on the slides coated with normal melting agarose (1%) and low melting point agarose was added as the top layer. The slides were immersed in lysis solution in the dark overnight (8 mM Tris–HCl, 2.5 M NaCl, 100 mM EDTA disodium salt dihydrate, 1% TRITON X-100 and 10% DMSO, pH 10, 4 °C). For the unwinding, the slides were immersed in alkaline electrophoresis buffer (20 min) (1 mM EDTA, 300 mM NaOH, 10% DMSO, pH > 13) and the electrophoresis was carried out in the same buffer (20 min, 1 V/cm and 300 mA). The slides were washed with neutralization buffer (0.4 M Tris-HCl, pH 7.5, 4 °C, 3 min), fixed with ethanol 70% (−20 °C, 5 min) and air dried. All steps were performed under yellow light to prevent additional DNA damage. Slides were stained with ethidium bromide (20 µg/ml) and analyzed using a fluorescence microscope (Axioskop HBO 50, Zeiss). The percentage of tail intensity was used to estimate DNA damage. A total of a hundred randomly selected cells per treatment (two gels per slides) were analyzed using the Comet Assay IV software (Perceptive Instruments, Instem). Two independent experiments were performed for each experimental condition.

Genotoxic effect (direct DNA damage) was evaluated comparing cells exposed to NPs with control cells (DMSO 1%). The formamidopyrimidine glycosylase (Fpg)-modified Comet assay was performed for DNA damage evaluation (direct + indirect DNA damage) as reported in Bonetta et al. (2009) with slight modification (Gea et al., 2018). The test was carried out as described for the alkaline Comet assay but, after lysis, the slides were washed with Fpg Buffer (5 min for three times) (40 mM Hepes, 0.1 M KCl, 0.5 mM EDTA disodium salt dihydrate, 0.2 mg/ml bovine serum albumin, pH 8). Then, each gel was incubated with 1 unit of Fpg enzyme (*Escherichia coli*) (Trevigen) at 37 °C for 30 min. Procedure control slides were incubated with buffer only. Cells treated with DMSO (1%) and enzyme were used as negative controls. Two independent experiments were performed for each experimental condition. The DNA damage (direct + indirect DNA damage) was evaluated comparing cells exposed to NPs with control cells (DMSO 1% + Fpg). The oxidative damage was calculated subtracting the mean tail intensity (%) in enzyme-treated cells (+Fpg) from the relative mean tail intensity (%) in enzyme-untreated cells (-Fpg).

2.8. 3D confocal micro-Raman imaging spectroscopy

Raman grade Calcium fluoride (CaF_2) windows (Crystran) were employed as alternative substrate instead of standard plastic substrates for cells growing due to the low toxicity and almost absent background signals (Kann et al., 2015). The BEAS-2B cells were cultured overnight

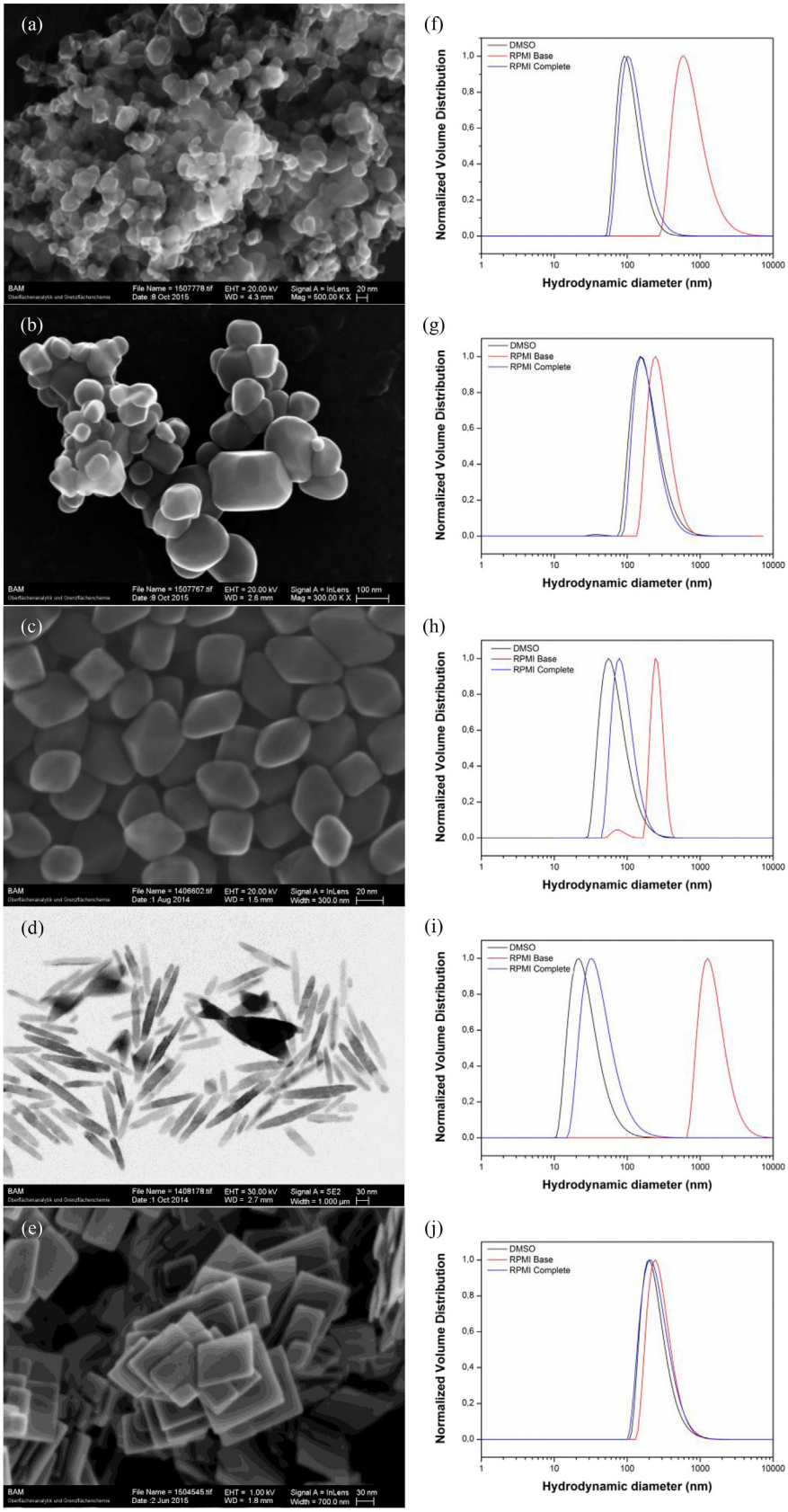

Fig. 1. SEM In-lens micrographs: (a) P25, (b) food grade, (c) bipyramids; (e) platelet NPs. T-SEM micrograph of rods (d). DLS analyses, normalized by volume distribution (f–j): (f) P25, (g) food grade, (h) bipyramids, (i) rods and (j) platelet NPs, suspensions in DMSO 1% (black line), base RPMI (red line) and complete RPMI (blue line). (For interpretation of the references to color in this figure legend, the reader is referred to the Web version of this article.)

in 6-well plates on a CaF_2 substrate (3×10^5 cells/well) before exposure to NPs. Cells were treated with NPs (80 μg/ml, 24 h). After exposure, cells were washed twice with PBS and fixed with 3 ml of methanol. CaF_2 substrates were dried and stained with Giemsa dye (4% Giemsa's azur eosin methylene blue solution, 4% Sorensen buffer 0.067 M pH 6.8, 8 min at room temperature); then the substrates were washed twice with distilled water and dried. Giemsa staining is one of the standard procedures in histology, useful to evidence morphological cells features, such as cell nuclei, which appear in various shades of red/purple, and the cytoplasm, which appears blue.

3D confocal micro-Raman imaging spectroscopy of BEAS-2B cells was conducted with a DXR™xi Raman Imaging Microscope (Thermo Scientific) using a laser wavelength at 532 nm, a 1 mW laser power, a 100X microscope objective and a motorized stage with a 1 μm of step size and a 1 μm offset. Spectra were collected in the 50–3500 cm^{-1} spectral region with a grating resolution of 5 cm^{-1}, an exposure time of 0.025 s and 5 scans in total. 3D Raman images were reconstructed taking the Raman peaks at 1600 cm^{-1} of methylene blue and the E_g band at 144 cm^{-1} of the TiO_2-NPs, respectively. Each cell was investigated at different focal planes and a chemical image was obtained by the combination of the ν(C-C)ring at 1600 cm^{-1} of the methylene blue and the Eg band at 144 cm^{-1} of the TiO_2-NPs. Since methylene blue is contained in the Giemsa stain and it is widely distributed into the fixed cells, its signals were considered representative of the entire volume of the cells. As far as the tracking of the NPs are concerned, the Eg band at 143 cm^{-1} is the most intense signal in the molecular fingerprint of the anatase TiO_2 and the region between 50 cm^{-1} and 400 cm^{-1} in the Raman spectrum is usually free of the vibrational bands of biological species. Therefore, this signal was selected to sensitively locate the TiO_2-NPs inside the cells. Image J software was used in the development of the 3D chemical images both for cells and TiO_2-NPs, which were superimposed using a Solidworks® 2016 Cad based software. 3D Raman chemical images are presented using a color meshwork i.e. blue for cell tissues and red for TiO_2 agglomerates.

2.9. Statistical analysis

IBM SPSS software (ver. 24.0) was used to perform statistical analysis. The results of WST-1, LDH and Comet assays are presented as the mean ± standard deviation. Differences between exposed and control cells were tested by ANOVA followed by the post hoc Dunnett's test. Differences between light and dark exposure were tested by ANOVA, followed by the post hoc Tukey's test. Data were considered statistically different for a p-value less than 0.05.

3. Results

3.1. Raman characterization of NPs and size distribution

In order to establish a relationship among the physico-chemical features of NPs and their ability to induce a toxic effect, well-defined and controlled protocols were developed for the production of engineered anatase TiO_2-NPs with different shapes. All the NPs produced in this study were first characterized with a SEM equipped with a transmission-unit for T-SEM, which provided information both on the shape and the size of the constituent NPs (Fig. 1a–e). Fig. 1 and Table 1 show shapes and particle size of commercial TiO_2-NPs and fabricated engineered TiO_2-NPs.

These NPs were also characterized by Dynamic Light Scattering (DLS) as a quick method for sizing and determining the state of NP agglomeration. For each kind of sample, the agglomeration in 1% DMSO aqueous solution, in base RPMI [supplemented with l-glutamine (4 mM) and penicillin-streptomycin (100 U/ml - 100 μg/ml)] and complete RPMI [supplemented with FBS (10% v/v), l-glutamine (4 mM) and penicillin-streptomycin (100 U/ml - 100 μg/ml)] (Fig. 1f–j) were compared. In all the TiO_2 materials considered for this study, the agglomeration state increase in base RPMI, while the size distribution in DMSO and in complete RPMI is quite similar.

The crystalline composition of the TiO_2-NPs, analyzed by Raman spectroscopy, showed a typical fingerprint of the anatase TiO_2 (Fig. S1) with the characteristic phonon bands E_g at 143 cm^{-1}, E_g at 197 cm^{-1}, A_{1g} at 397 cm^{-1}, B_{1g} at 515 cm^{-1} and E_g at 639 cm^{-1} for all the investigated NPs. Since P25 is a known mixture of anatase and rutile (5:1), with also a small amount of amorphous TiO_2 (Ohtani et al., 2010), its Raman spectrum still retains all the typical anatase Raman bands but it also contains two small shoulders at 450 cm^{-1} and 600 cm^{-1}, which were assigned to the E_g and A_{1g} phonon bands, respectively, of rutile (Tompsett et al., 1995). All the physiochemical properties of the TiO_2-NPs under study such as shape, particle size, hydrodynamic diameter in different liquid media and the crystalline phase are summarized in Table 1.

3.2. Cytotoxicity

The results of the effects of different TiO_2-NPs concentration on cell viability (WST-1 assay) are reported in Fig. 2a (exposure with light) and in Fig. 2b (exposure in darkness).

In general, a low cytotoxic effect was observed at the tested doses both in the exposure with light and in the exposure in darkness. The observed viability ranged from 102.8 to 88.4% for the exposure with light and from 99.6 to 87.4% for the exposure in darkness.

Considering the exposure with light, the commercial P25 induced a slight decrease in viability starting from the doses of 50 μg/ml ($p < 0.05$) while no cytotoxic effects were observed for the other commercial NPs (food grade) at the tested concentrations. As far as engineered NPs are concerned, bipyramids and platelet NPs induced the same cytotoxic effect of commercial P25 NPs; on the contrary, rods is the shape with higher cytotoxic effect showing a viability decrease already starting from 10 μg/ml ($p < 0.05$ or $p < 0.001$).

Considering the exposure in darkness, a lower cytotoxic effect was observed for commercial P25 NPs with respect to light exposure because a slight decrease in viability was observed for P25 NPs only at the highest dose (80 μg/ml) ($p < 0.05$). As reported after exposure with light, no cytotoxic effect was observed for the other commercial NPs (food grade). About engineered NPs, the exposure in darkness did not modify the cytotoxic effect of bipyramids resulting in a viability reduction starting from the dose of 50 μg/ml ($p < 0.001$) as reported in the experiment with light. In contrast, in the darkness, rods showed a lower cytotoxic effect than observed with light because a slight decrease in viability was observed for rods only starting from the dose of

Table 1
Physico-chemical properties of the TiO_2-NPs samples. Data are presented as mean ± standard deviation of 500 NPs for the particle size and 5 measurements for the hydrodynamic diameter (D_h) of each sample. *The particle size was calculated along the major axis of the NPs.

Sample	Particle size (nm)	D_h DMSO (nm)	D_h base RPMI (nm)	D_h complete RPMI (nm)	Crystalline phase
P25	20 ± 5 quasi-spherical	107 ± 31	722 ± 246	121 ± 37	anatase:rutile (5:1)
Food grade	150 ± 50 undefined shape	184 ± 61	278 ± 54	184 ± 55	anatase
Bipyramids	50 ± 9* (aspect ratio 3:2)	66 ± 20	259 ± 46	88 ± 24	anatase
Rods	108 ± 47* (aspect ratio 1:5)	36 ± 12	1500 ± 471	39 ± 17	anatase
Platelets	75 ± 25* (aspect ratio 8:1)	233 ± 70	281 ± 83	250 ± 82	anatase

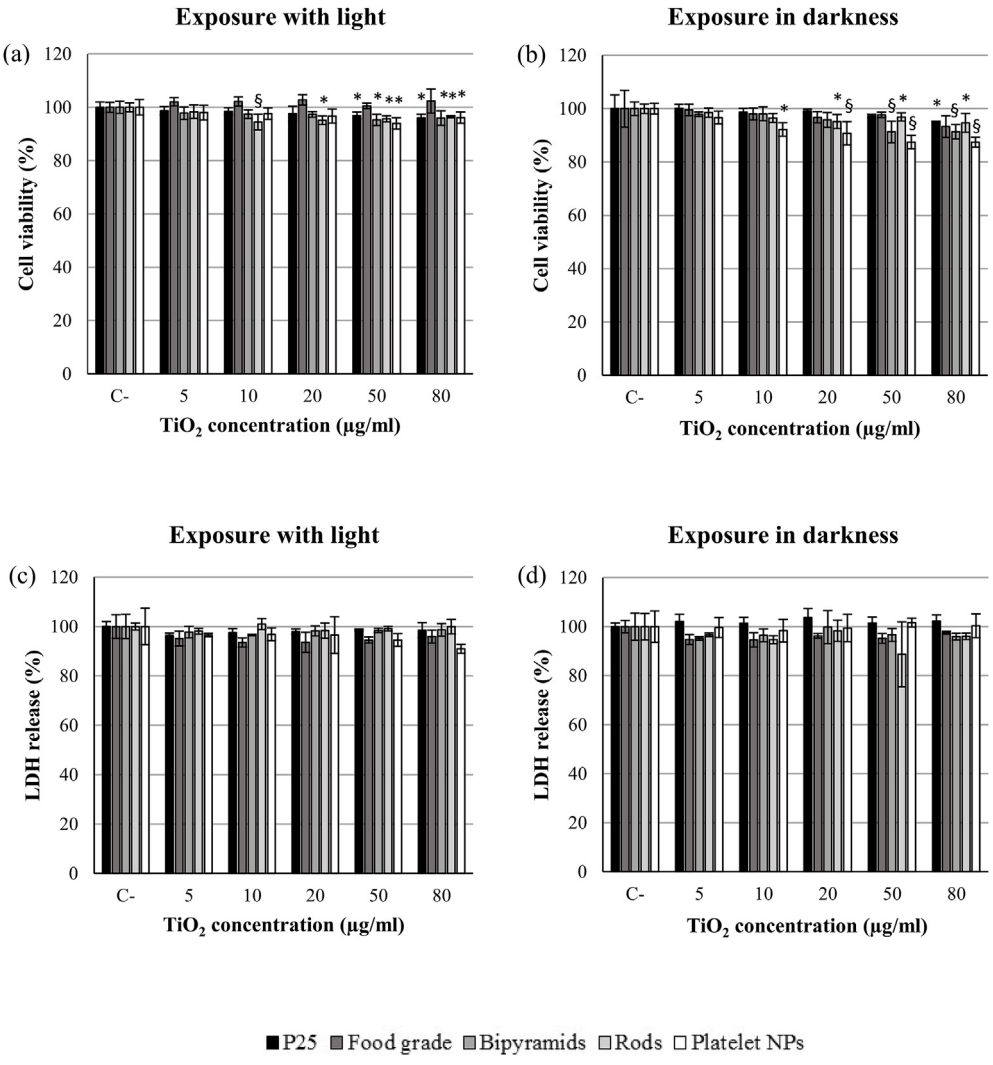

Fig. 2. Cytotoxicity measured with WST-1 (a,b) and LDH release (c,d) of BEAS-2B cells exposed to different concentrations (5–80 µg/ml) of commercial and engineered NPs. Control level is at 100%. Data represent effects detected after exposure with laboratory light (a,c) and in darkness (b,d). Data represent the mean % of the different wells, bars represent standard deviation. * = $p < 0.05$, § = $p < 0.001$ *vs* control cells (C-) according to ANOVA test, followed by the post hoc Dunnett's test.

20 µg/ml ($p < 0.05$). As during the exposure with light, platelet NPs induced a decrease in viability; the cytotoxic effect was significant starting from a less dose (10 µg/ml, $p < 0.05$) than in the experiment with light (50 µg/ml).

The results of the effects of different TiO_2-NPs concentration on LDH release has been reported in Fig. 2c (exposure with light) and in Fig. 2d (exposure in darkness).

No significant LDH release was detected using LDH assay in both exposure protocols (with light or in darkness), confirming the low cytotoxic effect evidenced by WST-1 assay.

3.3. Genotoxicity

The results of genotoxic effect and oxidative DNA damage induced by different concentration of NPs are reported in Fig. 3.

Considering the exposure with laboratory light, no genotoxic effect was showed in enzyme untreated cells (direct DNA damage) for commercial P25 NPs (Fig. 3a). On the other hand, a dose-dependent increase of DNA damage was observed for these NPs in enzyme treated cells (direct and indirect DNA damage) respect to the control cells ($p < 0.05$ or $p < 0.001$), with the exception of the last dose (160 µg/ml) that induced a DNA damage equal to 80 µg/ml. A significant oxidative damage was observed for P25 NPs starting from 50 µg/ml ($p < 0.05$ or $p < 0.001$). The results obtained with the other commercial NPs (food grade) (Fig. 3b) showed the presence of a significant dose-response DNA damage both in enzyme untreated cells and in enzyme treated cells starting from 50 µg/ml. Moreover, the difference between the two effects resulted significant starting from 50 µg/ml ($p < 0.05$ or $p < 0.001$) highlighting an oxidative damage induced by food grade NPs.

Respect to commercial NPs, engineered NPs showed a lower extent of DNA damage. In particular, neither genotoxic effect nor oxidative damage were observed for engineered bipyramids and rods NPs (Fig. 3c and d). Platelet NPs induced a significant DNA damage respect to the control cells ($p < 0.05$ or $p < 0.001$) both in enzyme untreated cells and in enzyme treated cells and they induced a significant oxidative DNA damage starting from 80 µg/ml ($p < 0.001$) (Fig. 3e). However, in contrast with commercial NPs (food grade), a dose-response of the effects were not observed.

As demonstrated by other authors (Karlsson, 2010; Karlsson et al., 2015), an interference during the scoring of the assay was detected in particular at the higher doses of P25 and platelet NPs, indeed nanoparticles with some autofluorescence were visible in the comets "head" and the stained DNA appeared faded. The interference probably caused

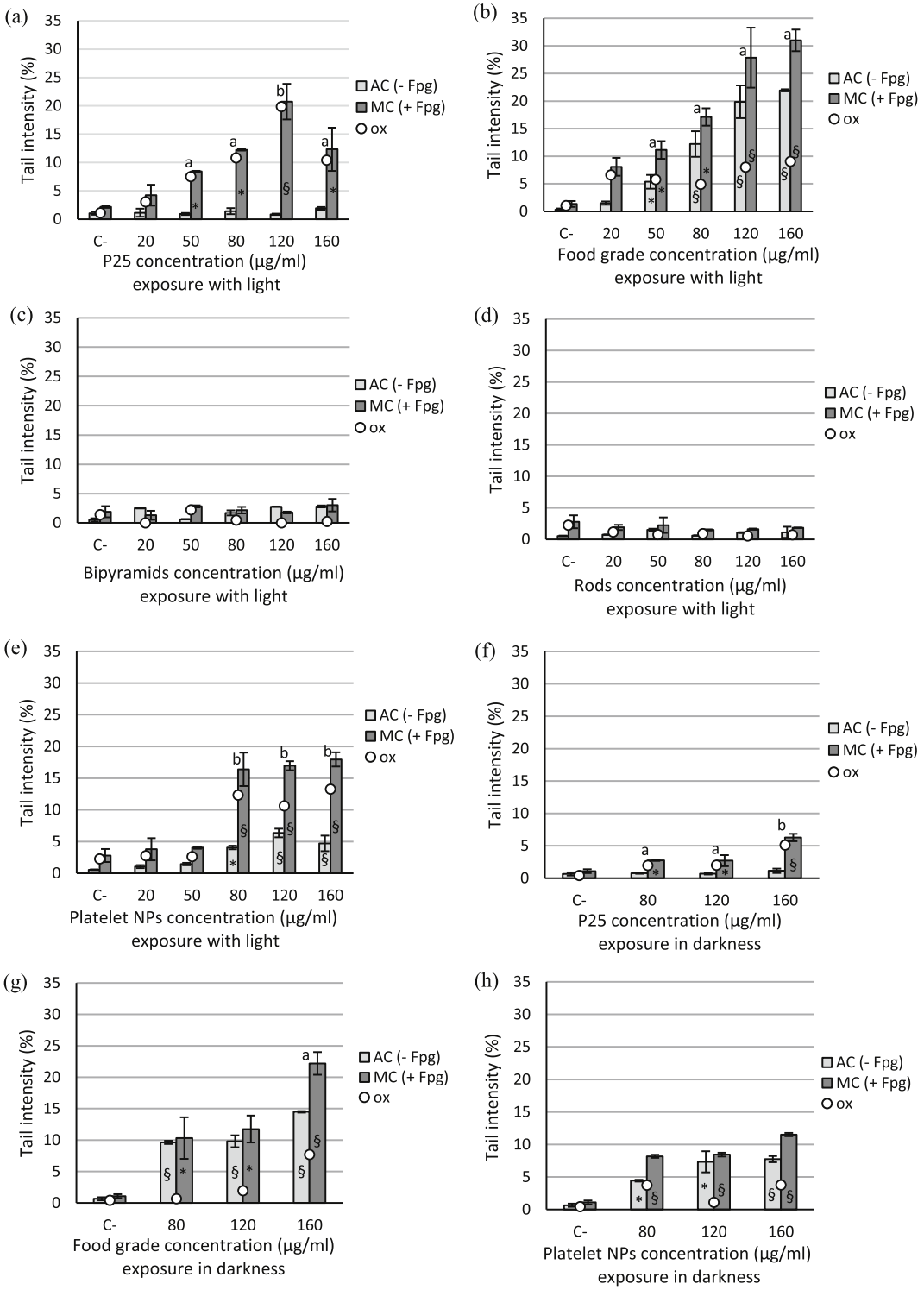

Fig. 3. Effect of BEAS-2B cells exposure to commercial and engineered NPs. AC (-Fpg) = alkaline Comet assay (direct DNA damage); MC (+Fpg) = Fpg-modified Comet assay (direct + indirect DNA damage). Ox = oxidative DNA damage (tail intensity (%) in enzyme-treated cells - tail intensity (%) in enzyme-untreated cells). Exposure with laboratory light (a–e): (a) P25, (b) food grade, (c) bipyramids, (d) rods, (e) platelet NPs; exposure in darkness (f–h): (f) P25, (g) food grade, (h) platelet NPs. Data represent the mean % of tail intensity; bars represent standard deviation of two independent experiments for each experimental condition. * = $p < 0.05$, § = $p < 0.001$ DNA damage *vs* control cells (C-). a = $p < 0.05$, b = $p < 0.001$ oxidative DNA damage *vs* control cells (ox C-). According to ANOVA test, followed by the post hoc Dunnett's test.

the loss of concentration-dependent increase in DNA direct and oxidative damage observed for the higher doses. The phenomenon could be explained also considering that base oxidation is hard to measure accurately when there are a lot of strand breaks, because the Comet assay becomes saturated (Collins et al., 2017).

In order to evaluate the role of the light on the genotoxic and oxidative damage induced by commercial and engineered NPs, the highest doses (80, 120, 160 μg/ml) of NPs that showed a genotoxic effect (P25, food grade and platelet NPs) were tested in darkness (24 h).

Considering the exposure in darkness, no genotoxic effect was

observed for commercial P25 NPs in enzyme untreated cells (direct DNA damage) (Fig. 3f) as reported in the experiment with light (Fig. 3a). However, in the enzyme treated cells a dose-response DNA damage (direct and indirect DNA damage) was observed with respect to control cells ($p < 0.05$ or $p < 0.001$), but oxidative DNA damage was lower than in the experiment with light ($p < 0.05$ or $p < 0.001$). The commercial food grade NPs induced a significant dose-response DNA damage both in enzyme untreated cells and in enzyme treated cells ($p < 0.001$ and $p < 0.05$ respectively) (Fig. 3g). However, the DNA damage resulted in both cases lower than in the experiment with light ($p < 0.05$ or $p < 0.001$) and an oxidative damage was induced only at the highest dose (160 µg/ml) ($p < 0.05$).

With regard to engineered NPs, platelet NPs induced a significant DNA damage with respect to the control cells ($p < 0.05$ or $p < 0.001$)

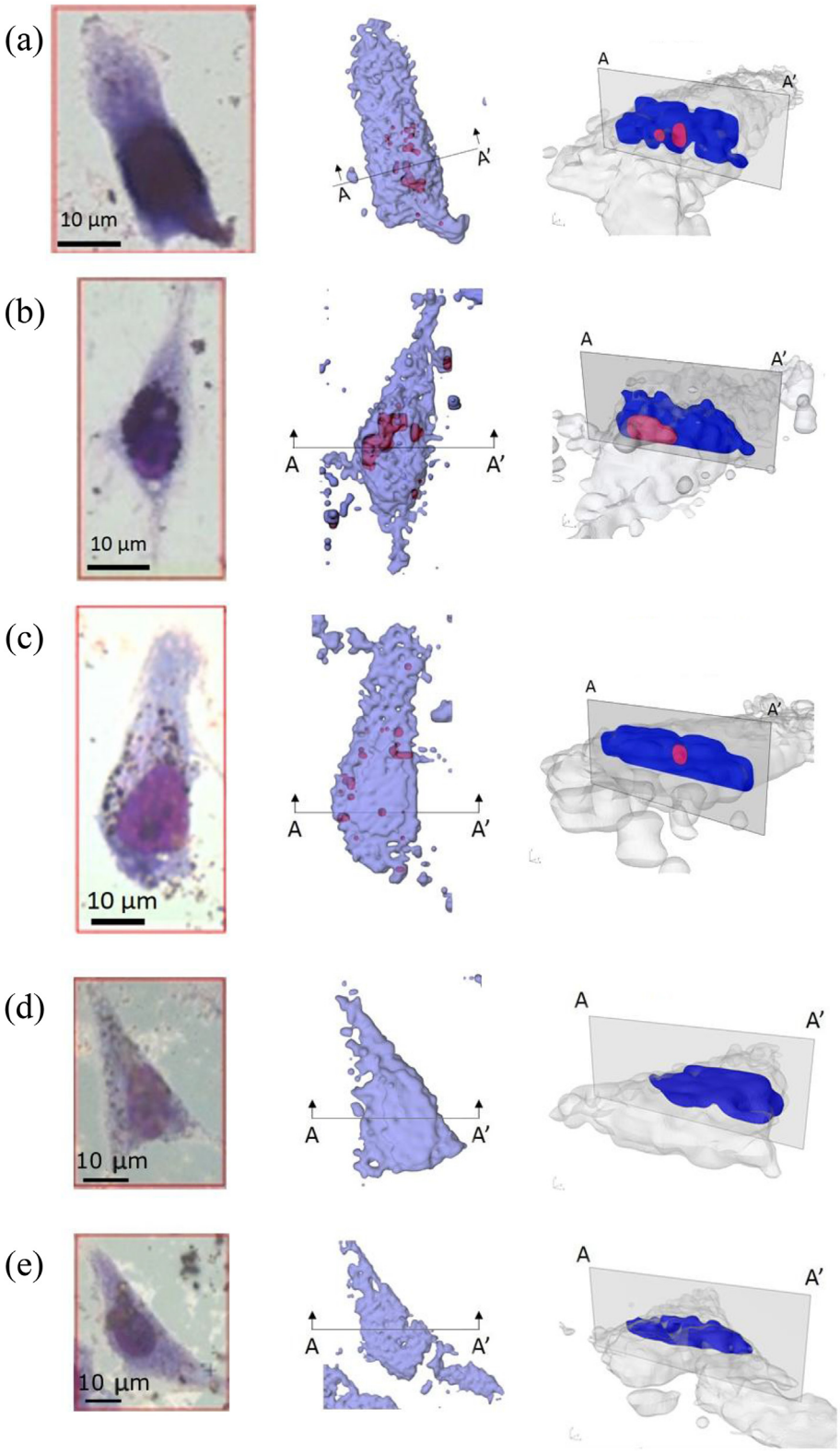

Fig. 4. 3D confocal micro-Raman imaging of BEAS-2B cells after exposure to commercial and engineered NPs. Top views (optical and 3D Raman) and 3D Raman sections are shown from the left to the right: (a) P25, (b) food grade, (c) platelet NPs, (d) bipyramids, (e) rods. 3D chemical images are built by superimposing the different maps of each cell at their corresponding focal planes and they are presented using a color meshwork i.e. blue for cell tissues (methylene blue ν(C-C)ring at 1600 cm^{-1}) and red for TiO_2 agglomerates (Eg band at 144 cm^{-1} of the anatase TiO_2). (For interpretation of the references to color in this figure legend, the reader is referred to the Web version of this article.)

both in enzyme untreated cells and in enzyme treated cells (Fig. 3h). However, while the DNA damage in enzyme untreated cells was equivalent to the DNA damage induced in the experiment with light (Fig. 3e), a decrease of DNA damage in enzyme treated cells was observed, resulting in no oxidative damage induced by platelet NPs in darkness (Fig. 3h).

3.4. Confocal micro-Raman spectroscopy

The confocal micro-Raman imaging spectroscopy was used in order to evaluate qualitatively the presence/absence of different types of TiO_2-NPs inside the cells. 3D chemical images are built by superimposing the different maps of each cell at their corresponding focal planes and they are presented using a color meshwork i.e. blue for cell tissues and red for TiO_2 agglomerates. At least five cells were analyzed to provide statistically significant results. As the sections of Fig. 4 show, the uptake of the TiO_2-NPs by the cells was mainly demonstrated for P25, food grade and platelet NPs (Fig. 4a,b,c) while no TiO_2 signal was registered inside the cells for bypiramids and rods (Fig. 4d and e).

4. Discussion

Many *in vitro* studies have been conducted to investigate cytotoxicity/genotoxicity of TiO_2-NPs but the results are often conflicting and employed doses were sometimes high (Valant et al., 2012; Chen et al., 2014; Magdolenova et al., 2014; Karlsson et al., 2015; Moller et al., 2015a). The aim of this study was to investigate the cytotoxicity and genotoxicity of three different shapes of TiO_2-NPs and to compare them with two commercial TiO_2-NPs.

The issues taken into account for this study were: i) the physicochemical properties of the particles (shape, particle size, agglomeration state in culture media, crystalline phase) that can influence biological effects, ii) the ability of the particles to induce cytotoxicity and genotoxicity, iii) the increase of the toxicological effects under light exposure due to the photocatalytic activity of TiO_2 and iv) the uptake of the NPs by human cells.

In the present study, the cytotoxicity assays were selected in order to reduce the interference of NPs with the assays (interference with optical detection methods, ability to convert the substrates). As suggested by other studies (Wilhelmi et al., 2012; Guadagnini et al., 2015: Popescu et al., 2015), the assays processes were optimized for evaluation of NPs; moreover, before the assessment of NPs cytotoxicity, relevant controls were conducted, in order to assess particles for their ability to interfere with the assays (data not shown).

For genotoxicity evaluation, a literature revision (on application of genotoxicity assays testing NPs) was made before the application of Comet assay (Karlsson, 2010; Magdolenova et al., 2012a; Karlsson et al., 2015; Cowie et al., 2015; Moller et al., 2015b; Huk et al., 2015). To ensure the correct evaluation of DNA damage two independent experiment were performed for each experimental condition. The analysis of each comet was made using the Comet Assay IV software and the automatic evaluation was carefully checked by an operator.

Published results on toxicity of TiO_2-NPs show high variability. Reasons for this variability include physico-chemical characteristics of NPs, different methods to prepare NPs dispersions, differences in NPs size and dispersion stability, and different exposure protocols (Charles et al., 2018). The characteristics of NPs dispersion can be influenced by medium components, such as serum proteins, and by NPs properties (i.e. size, shape, surface charge, surface coating) (Huk et al., 2015). According to the study of Prasad et al. (2013), the present results showed that in all the TiO_2-NPs dispersions, the agglomeration state increases in base RPMI (without serum), while the size distribution in DMSO and in complete RPMI medium (with serum) is quite similar. The different agglomeration state is probably due to the ability of metal oxide NPs to adsorb proteins onto their surface, forming a “protein corona” which favors less agglomeration in complete medium, which contains more proteins (Prasad et al., 2013). Considering the results obtained, complete medium was selected as cytotoxicity/genotoxicity assay medium.

The viability of BEAS-2B treated with commercial and engineered TiO_2-NPs after exposure with light or in darkness was assessed using the WST-1 assay.

Commercial TiO_2-NPs induced low (P25) or no viability reduction (food grade) detected by WST-1 assay; these results are in agreement with some reports on commercial TiO_2-NPs (Bhattacharya et al., 2009; Falck et al., 2009). Previous studies that investigated the cytotoxicity of commercial P25 on BEAS-2B showed that only 100 μg/ml of commercial P25 NPs produced a viability decrease after 24 h exposure (Prasad et al., 2013). Fewer studies have been performed using commercial food grade TiO_2-NPs. Proquin et al. (2017) tested these NPs on different cell lines: on Caco-2, they observed cytotoxicity, while on HCT116 they did not observe any cytotoxic effect up to the concentration of 100 μg/cm^2. The result obtained on HCT116 was in accordance with the low cytotoxic effect induced by commercial food grade TiO_2-NPs detected in the present study. Recently, the scientific community have produced reference NPs, which have been well characterized. Di Bucchianico et al. (2016) assessed cytotoxic effects of some of these NPs (anatase 50–150 nm, anatase 5–8 nm, rutile 20–28 nm) in BEAS-2B cells and, according to the present results, showed in general no or low effects at the tested doses (2–100 μg/ml).

On the contrary, other studies showed that commercial TiO_2-NPs induced higher cytotoxicity on BEAS-2B (Shi et al., 2010; Ursini et al., 2014). In particular, Park et al. (2008) found that exposure of BEAS-2B cells to commercial P25 (5–40 μg/ml) for 24 h led to significant cell death, both in a time- and concentration-dependent manner.

The data of present study demonstrated that cytotoxicity was slightly affected by light exposure, which induced an increase of cellular damage after incubation with commercial P25 and engineered rods. The influence of light exposure on citotoxicity was also observed in other studies (Vevers and Jha, 2008; Reeves et al., 2008). Differently from P25 and rods, exposure to platelet NPs induced higher cytotoxicity in darkness than after light exposure; the mechanism that led to this result is not clear.

Comparing the results of cytotoxicity (WST-1 assay) and LDH release, the first showed low cytotoxic effect at the doses tested, while the second did not show any cytotoxicity in both exposure protocols. The discrepancy between cytotoxicity (WST-1) and LDH release suggests that the viability reduction may be caused by apoptosis, a cell death pathway in which the plasma membrane is maintained, as observed in other studies (Schilirò et al., 2015). This is in accordance with previous studies, which demonstrated that TiO_2-NPs could cause apoptosis in BEAS-2B cells (Park et al., 2008; Shi et al., 2010). The observed discrepancy could be also explained considering that the tested compounds (TiO_2-NPs) could induce an effect on the intracellular activity (mitochondrial activity) without causing plasma membrane breakage, as observed by other authors (Weyermann et al., 2005; Fotakis and Timbrell, 2006).

Results of Comet assay in presence of light and in darkness showed a significant DNA damage induced by commercial P25 and food grade NPs and engineered platelet NPs, while no genotoxicity was observed with the other engineered NPs (bipyramids and rods).

Considering that the uptake of NPs could involve interactions of NPs with DNA, the observed genotoxic effect could be related to the presence of P25, food grade and platelet NPs into the BEAS-2B as observed by other authors (Bhattacharya et al., 2009; Park et al., 2008).

In the present study, the higher uptake of P25, food grade and platelet NPs seemed to be related with higher agglomeration tendency (higher measure of hydrodynamic diameter) (Table 1). In particular, the engineered platelet NPs were the most agglomerated (platelet shape could probably promote more agglomeration than the other shapes) and commercial P25 and food grade were more agglomerated than the other engineered NPs (bipyramids and rods). The variation in cellular

uptake could be due to agglomeration tendency because NPs that form large agglomerates, differently from NPs that form smaller ones, precipitate at the bottom of the cell culture wells, increasing the real amount of NPs to which cells are exposed (Magdolenova et al., 2012b). Cells exposed to more NPs could probably internalize more NPs.

Then, in the present study, the agglomeration tendency does not seem to have prevented the uptake of NPs in the cells, in accordance with the study of Ahlinder et al. (2013).

The major uptake of P25, food grade and platelet NPs could be related with higher genotoxic effect considering that, after penetration into the cells, NPs may have direct access to DNA via transport into the nucleus and/or during mitosis when the dissolution of nuclear membrane occurs. NPs interacting directly with DNA could cause DNA breakage (Magdolenova et al., 2014). Moreover, NPs, after penetration into the cells, can enhance the permeability of the lysosomal membrane, inducing the release of DNases and so causing genotoxic effects (Karlsson, 2010). Finally, accumulation of NPs within cells can cause aggregates of NPs that deform nucleus inducing DNA damage (Di Virgilio et al., 2010).

In order to quantify effects due to the photocatalytic activity of TiO_2, the highest doses (80, 120, 160 μg/ml) of NPs that showed a genotoxic effect were tested also in darkness (24 h). Results obtained in this study showed that light exposure induced additional indirect genotoxicity, demonstrating a higher oxidative potential of TiO_2-NPs after exposure with light. The presence of light increased DNA oxidative damage probably due to the photocatalytic activity of TiO_2-NPs, which caused an increase of NPs ability to produce radicals. In particular, based on previous studies, the anatase crystal structure of TiO_2 (the same used in the present study) seems to be the most catalytic/photocatalytic crystalline structure of TiO_2 and seems to be activated under both ultraviolet and visible light (Warheit and Donner, 2015). A recent study (De Matteis et al., 2016) demonstrated that, in particular using anatase, light is a dominant factor to induce oxidative stress and toxic effects. Also Gerloff et al. (2009) showed the increase of oxidative genotoxic effects induced by TiO_2-NPs (80%/20% anatase-rutile) in the presence of interior light.

However, an oxidative damage (although low) was observed in the present study also in darkness as reported in the study of Gurr et al. (2005) that demonstrated that in darkness TiO_2-NPs can induce oxidative DNA damage. On the contrary, Karlsson et al. (2008) and Gerloff et al. (2009) found that TiO_2-NPs (mixture of rutile and anatase) in darkness did not show oxidative DNA damage using the Fpg-modified Comet assay.

Moreover, the results obtained in this study highlight that only food grade and platelet NPs induced direct genotoxicity. However, while for food grade NPs the direct genotoxic effect remains the same both after exposure with light and in the darkness, for the commercial food grade NPs, the direct damage was higher in presence of light than in darkness. This result agree with the study of Gopalan et al. (2009); they suggest that TiO_2 (anatase 40–70 nm range) is capable of inducing higher direct genotoxic effects after simultaneous irradiation with UV, respect to genotoxicity induced in darkness. The increase of direct DNA damage after exposure with light attested by Gopalan et al. (2009) and detected for food grade NPs, remain to be explained. A possible mechanism that may lead to this effect could be related to the potential interaction of TiO_2-NPs with proteins involved in DNA repair, as demonstrated by Jugan et al. (2011). Genotoxicity is not only linked to the level of DNA damage but also to the type of lesions generated and their capacity to be repaired. NPs exposure in presence of light could influence activity of proteins such as repair enzymes, resulting in DNA damage not repaired or misrepaired (Magdolenova et al., 2014). Then, the exposure with light may have caused inactivation of repair enzymes, inducing a higher direct genotoxic effect induced by food grade NPs after exposure with light respect to exposure in darkness.

In conclusion, the results of this study showed that the cytotoxicity was overall low (WST-1 assay) and was influenced by the NP shape as well as by light exposure. According to the low cytotoxic effect, no LDH release was detected using the LDH assay.

Instead, genotoxicity seemed to be influenced by the cellular-uptake and the aggregation tendency of TiO_2-NPs. These two aspects are probably related to different physico-chemical characteristics of NPs, such as the shape. Moreover, the presence of light enhanced the genotoxic effect of some NPs primarily increasing the oxidative stress.

Although more studies have to be performed in order to assess the potential toxicity of engineered NPs, the results of this preliminary study showed that engineered NPs did not induced a high cytotoxic/genotoxic effect compared to the other commercial TiO_2-NPs, so they could be used for future technological applications. The results of this study are important considering that engineered NPs, due to their peculiar characteristics, could support and improve TiO_2-NPs applications in different areas such as energy (i.e. use of engineered TiO_2-NPs in dye-sensitized solar cells), environment (i.e. application of engineered TiO_2-NPs as photocatalyst for the abatement of air and water pollutants) and health (i.e. use of engineered TiO_2-NPs for the production of nanostructured coatings of orthopedic and dental prostheses exhibiting optimized interfacial properties).

Conflicts of interest

The authors declare that they have no competing interests.

Appendix A. Supplementary data

Supplementary data to this article can be found online at https://doi.org/10.1016/j.fct.2019.02.043.

Funding

This work was supported by the SETNanoMetro Seventh Framework Programme project (project number 604577; call identifier FP7-NMP-2013_LARGE-7).

References

Ahlinder, L., Ekstrand – Hammarstrom, B., Geladi, P., Osterlund, L., 2013. Large uptake of titania and iron oxide nanoparticle in the nucleus of lung epithelial cells as measured by Raman imaging and multivariate classification. Biophys. J. 105, 310–319. https://doi.org/10.1016/j.bpj.2013.06.017.

Allegri, M., Bianchi, M.G., Chiu, M., Varet, G., Costa, A.L., Ortelli, S., Blosi, M., Bussolati, O., Poland, C.A., Bergamaschi, E., 2016. Shape-related toxicity of titanium dioxide nanofibres. PLoS One 11 (3), 1–21. https://doi.org/10.1371/journal.pone.0151365.

Bernard, A.S., Curtiss, L.A., 2005. Prediction of TiO_2 nanoparticle phase and shape transitions controlled by surface chemistry. Nano Lett. 5, 1261–1266. https://doi.org/10.1021/nl050355m.

Bhattacharya, K., Davoren, M., Boertz, J., Schins, R.P., Hoffmann, E., Dopp, E., 2009. Titanium dioxide nanoparticles induce oxidative stress and DNA-adduct formation but not DNA-breakage in human lung cells. Part. Fibre. Toxicol. 6, 17–27. https://doi.org/10.1186/1743-8977-6-17.

Bonetta, S., Bonetta, S., Motta, F., Strini, A., Carraro, E., 2013. Photocatalytic bacterial inactivation by TiO_2–coated surfaces. Amb. Express 3, 59–66. https://doi.org/10.1186/2191-0855-3-59.

Bonetta, S., Bonetta, S., Schilirò, T., Ceretti, E., Feretti, D., Covolo, L., Vannini, S., Villarini, M., Moretti, M., Verani, M., Carducci, A., Bagordo, F., De Donno, A., Bonizzoni, S., Bonetti, A., Pignata, C., Carraro, E., Gelatti, U., MAPEC_LIFE Study Group,Gilli, G., Romanazzi, V., Gea, M., Festa, A., Viola, G.C.V., Zani, C., Zerbini, I., Donato, F., Monarca, S., Fatigoni, C., Levorato, S., Salvatori, T., Donzelli, G., Palomba, G., Casini, B., De Giorgi, M., Devoti, G., Grassi, T., Idolo, A., Panico, A., Serio, F., Furia, C., Colombi, P., 2019. Mutagenic and genotoxic effects induced by PM0.5 of different Italian towns in human cells and bacteria: the MAPEC_LIFE study. Environ. Pollut. 245, 1124–1135. https://doi.org/10.1016/j.envpol.2018.11.017.

Bonetta, S., Giannotti, V., Bonetta, S., Gosetti, F., Oddone, M., Carraro, E., 2009. DNA damage in A549 cells exposed to different extracts of PM2.5 from industrial, urban and highway sites. Chemosphere 77, 1030–1034. https://doi.org/10.1016/j.chemosphere.2009.07.076.

Charles, S., Jomini, S., Fessard, V., Bigorgne-Vizade, E., Rousselle, C., Michel, C., 2018. Assessment of the in vitro genotoxicity of TiO_2 nanoparticles in a regulatory context. Nanotoxicology 12 (4), 357–374. https://doi.org/10.1080/17435390.2018.1451567.

Chen, T., Yan, J., Li, Y., 2014. Genotoxicity of titanium dioxide nanoparticles. J. Food Drug Anal. 22, 95–104. https://doi.org/10.1016/j.jfda.2014.01.008.

Collins, A., El Yamani, N., Dusinska, M., 2017. Sensitive detection of DNA oxidation damage induced by nanomaterials. Free Radic. Biol. Med. 107, 69–76. https://doi.org/10.1016/j.freeradbiomed.2017.02.001.

Cowie, H., Magdolenova, Z., Saunders, M., Drlickova, M., Carreira, S.C., Kenzaoi, B.H., Gombau, L., Guadagnini, L., Lorenzo, Y., Walker, L., Fjellsbo, L.M., Huk, H., Rinna, A., Tran, L., Volkova, K., Boland, S., Jullierat- Jeanneret, L., Marano, F., Collins, A.R., Dusinska, M., 2015. Suitability of human and mammalian cells of different origin for the assessment of genotoxicity of metal and polymeric engineered nanoparticles. Nanotoxicology 9, 57–65. https://doi.org/10.3109/17435390.2014.940407.

De Matteis, V., Cascione, M., Brunetti, V., Toma, C.C., Rinaldi, R., 2016. Toxicity assessment of anatase and rutile titanium dioxide nanoparticles: the role of degradation in different pH conditions and light exposure. Toxicol. Vitro 37, 201–210. https://doi.org/10.1016/j.tiv.2016.09.010.

Di Bucchianico, S., Cappellini, F., Le Bihanic, F., Zhang, Y., Dreij, K., Karlsson, H.L., 2016. Genotoxicity of TiO_2 nanoparticle assessed by mini-gel Comet assay and micronucleus scoring with flow cytometry. Mutagenesis 32 (1), 127–137. https://doi.org/10.1093/mutage/gew030.

Di Virgilio, A.L., Reigosa, M., Arnal, P.M., Fernández Lorenzo de Mele, M., 2010. Comparative study of the cytotoxic and genotoxic effects of titanium oxide and aluminium oxide nanoparticles in Chinese hamster ovary (CHO-K1) cells. J. Hazard Mater. 177, 711–718. https://doi.org/10.1016/j.jhazmat.2009.12.089.

Falck, G.C.M., Lindberg, H.K., Suhonen, S., Vippola, M., Vanhala, E., Catalan, J., Savolainen, K., Norppa, H., 2009. Genotoxic effects of nanosized and fine TiO_2. Hum. Exp. Toxicol. 28 (6 – 7), 339–352. https://doi.org/10.1177/0960327109105163.

Fotakis, G., Timbrell, J.A., 2006. In vitro cytotoxicity assays: comparison of LDH, neutral red, MTT and protein assay in hepatoma cell lines following exposure to cadmium chloride. Toxicol. Lett. 160, 171–177. https://doi.org/10.1016/j.toxlet.2005.07.001.

Gea, M., Schilirò, T., Iacomussi, P., Degan, R., Bonetta, S., Gilli, G., 2018. Cytotoxicity and genotoxicity of light emitted by incandescent, halogen, and LED bulbs on ARPE-19 and BEAS-2B cell lines. J. Toxicol. Environ. Health 81 (19), 998–1014. https://doi.org/10.1080/15287394.2018.1510350.

Gerloff, K., Albrecht, C., Boots, A.W., Förster, I., Schins, R.P.F., 2009. Cytotoxicity and oxidative DNA damage by nanoparticles in human intestinal Caco-2 cells. Nanotoxicology 3 (4), 355–364. https://doi.org/10.3109/17435390903276933.

Gopalan, R.C., Osman, I.F., Amani, A., De Matas, M., Anderson, D., 2009. The effect of zinc oxide and titanium dioxide nanoparticles in the Comet assay with UVA photo activation of human sperm and lymphocytes. Nanotoxicology 3 (1), 33–39. https://doi.org/10.1080/17435390802596456.

Guadagnini, R., Halamoda Kenzaoui, B., Walker, L., Pojana, G., Magdolenova, Z., Bilanicova, D., Saunders, M., Juillerat-Jeanneret, L., Marcomini, A., Huk, A., Dusinska, M., Fjellsbo, L.M., Marano, F., Boland, S., 2015. Toxicity screenings of nanomaterials: challenges due to interference with assay processes and components of classic in vitro tests. Nanotoxicology 9, 13–24. https://doi.org/10.3109/17435390.2013.829590.

Gurr, J.R., Wang, A.S., Chen, C.H., Jan, K.Y., 2005. Ultrafine titanium dioxide particles in the absence of photoactivation can induce oxidative damage to human bronchial epithelial cells. Toxicology 213, 66–73. https://doi.org/10.1016/j.tox.2005.05.007.

Hamilton, R.F., Wu, N., Porter, D., Buford, M., Wolfarth, M., Holian, A., 2009. Particle length-dependent titanium dioxide nanomaterials toxicity and bioactivity. Part. Fibre Toxicol. 6, 35–46. https://doi.org/10.1186/1743-8977-6-35.

Han, X., Kuang, Q., Jin, M., Xie, Z., Zheng, L., 2009. Synthesis of titania nanosheets with a high percentage of exposed (001) facets and related photocatalytic properties. J. Am. Chem. Soc. 131 (9), 3152–3153. https://doi.org/10.1021/ja8092373.

Huk, A., Collins, A.R., El Yamani, N., Porredon, C., Azqueta, A., de Lapuente, J., Dusinska, M., 2015. Critical factors to be considered when testing nanomaterials for genotoxicity with the comet assay. Mutagenesis 30, 85–88. https://doi.org/10.1093/mutage/geu077.

Iannarelli, L., Giovannozzi, A.M., Morelli, F., Viscotti, F., Bigini, P., Maurino, V., Spoto, G., Martra, G., Ortel, E., Hodoroaba, V., Rossi, A.M., Diomede, L., 2016. Shape engineered TiO_2 nanoparticles in *Caenorhabditis elegans*: a Raman imaging based approach to assist tissue-specific toxicological studies. RSC Adv. 6, 70501–70509. https://doi.org/10.1039/c6ra09686g.

IARC, 2010. Carbon black, titanium dioxide, and talc. IARC Monogr. Eval. Carcinog. Risks Hum. 93, 1–413.

International Standards Organisation (ISO), 2015. Nanotechnologies – Vocabulary – Part 2: Nano-Objects. ISO 80004-2, Geneva, Switzerland.

Johnston, H.J., Hutchison, G.R., Christensen, F.M., Peters, S., Hankin, S., Stone, V., 2009. Identification of the mechanisms that drive the toxicity of TiO_2 particulates: the contribution of physicochemical characteristics. Part. Fibre Toxicol. 6, 33. https://doi.org/10.1186/1743-8977-6-33.

Jovanovic, B., 2015. Critical review of public health regulations of titanium dioxide, a human food additive. Integr. Environ. Assess. Manag. 11, 10–20. https://doi.org/10.1002/ieam.1571.

Jugan, M.L., Barillet, S., Simon-Deckers, A., Herlin-Boime, N., Sauvaigo, S., Douki, T., Carriere, M., 2011. Titanium dioxide nanoparticles exhibit genotoxicity and impair DNA repair activity in A549 cells. Nanotoxicology 6 (5), 501–513. https://doi.org/10.3109/17435390.2011.587903.

Kann, B., Offerhaus, H.L., Windbergs, M., Otto, C., 2015. Raman microscopy for cellular investigations – from single cell imaging to drug carrier uptake visualization. Adv. Drug Deliv. Rev. 89, 71–90. https://doi.org/10.1016/j.addr.2015.02.006.

Karlsson, H.L., Cronholm, P., Gustafsson, J., Möller, L., 2008. Copper oxide nanoparticles are highly toxic: a comparison between metal oxide nanoparticles and carbon nanotubes. Chem. Res. Toxicol. 21, 1726–1732. https://doi.org/10.1021/tx800064j.

Karlsson, H.L., Di Bucchianico, S., Collins, A., Dusinska, M., 2015. Can the Comet Assay be used reliably to detect nanoparticle-induced genotoxicity? Environ. Mol. Mutagen. 56, 82–96. https://doi.org/10.1002/em.21933.

Karlsson, H.L., 2010. The Comet assay in nanotoxicology research. Anal. Bioanal. Chem. 398, 651–666. https://doi.org/10.1007/s00216-010-3977-0.

Lavric, V., Isopescu, R., Maurino, V., Pellegrino, F., Pellutiè, L., Ortel, E., Hodoroaba, A., 2017. New model for nano-TiO_2 crystal birth and growth in hydrothermal treatment using an oriented attachment approach. Cryst. Growth Des. 17 (11), 5640–5651. https://doi.org/10.1021/acs.cgd.7b00302.

Magdolenova, Z., Bilanicova, D., Pojana, G., Fjellsbo, L.M., Hudecova, A., Hasplova, K., Marcomini, A., Dusinska, M., 2012b. Impact of agglomeration and different dispersion of titanium dioxide nanoparticles on the human related in vitro cytotoxicity and genotoxicity. J. Environ. Monit. 14, 455–464. https://doi.org/10.1039/c2em10746e.

Magdolenova, Z., Collins, A., Kumar, A., Dhawan, A., Stone, V., Dusinska, M., 2014. Mechanisms of genotoxicity. A review of in vitro and in vivo studies with engineered nanoparticles. Nanotoxicology 8 (3), 233–278. https://doi.org/10.3109/17435390.2013.773464.

Magdolenova, Z., Lorenzo, Y., Collins, A., Dusinska, M., 2012a. Can standard genotoxicity tests be applied to nanoparticles? J. Toxicol. Environ. Health 75, 13–15. https://doi.org/10.1080/15287394.2012.690326.

Mohra, U., Ernst, H., Roller, M., Pott, F., 2006. Pulmonary tumor types induced in Wistar rats of the so-called 19-dust study. Exp. Toxicol. Pathol. 58 (1), 13–20. https://doi.org/10.1016/j.etp.2006.06.001.

Moller, P., Hemmingsen, J.G., Jensen, D.M., Danielsen, P.H., Karottki, D.G., Jantzen, K., Roursgaard, M., Cao, Y., Kermanizadeh, A., Klingberg, H., Christophersen, D.V., Hersoug, L., Loft, S., 2015a. Applications of the comet assay in particle toxicology: air pollution and engineered nanomaterials exposure. Mutagenesis 30, 67–83. https://doi.org/10.1093/mutage/geu035.

Moller, P., Jensen, D.M., Christophersen, D.V., Kermanizadeh, A., Jacobsen, N.R., Hemmingsen, J.G., Danielsen, P.H., Karottki, D.G., Roursgaard, M., Cao, Y., Jantzen, K., Klinberg, H., Hersoug, L., Loft, S., 2015b. Measurement of oxidative DNA damage to DNA in nanomaterial exposed cells and animals. Environ. Mol. Mutagen. 56, 97–110. https://doi.org/10.1002/em.21899.

National Institute for Occupational Safety and Health (NIOSH), 2011. Occupational exposure to titanium dioxide. In: Current Intelligence Bulletin 63. National Institute for Occupational Safety and Health, Cincinnati.

Numano, T., Xu, J., Futakuchi, M., Fukamachi, K., Alexander, D.B., Furukawa, F., Kanno, J., Hirose, A., Tsuda, H., Suzuim, M., 2014. Comparative study of toxic effects of anatase and rutile type nanosized titanium dioxide particles in vivo and in vitro. Asian Pac. J. Cancer Prev. APJCP 15 (2), 929–935. https://doi.org/10.7314/APJCP.2014.15.2.92.

Ohtani, B., Prieto-Mahaney, O.O., Li, D., Abe, R., 2010. What is Degussa (Evonik) P25? Crystalline composition analysis, reconstruction from isolated pure particles and photocatalytic activity test. J. Photochem. Photobiol., A 216, 179–182. https://doi.org/10.1016/j.jphotochem.2010.07.024.

Park, E.J., Lee, G., Shim, H., Kim, J., Cho, M., Kim, D., 2013. Comparison of toxicity of different nanorod-type TiO_2 polymorphs in vivo and in vitro. J. Appl. Toxicol. 34, 357–366. https://doi.org/10.1002/jat.2932.

Park, E.J., Yi, J., Chung, Y.H., Ryu, D.Y., Choi, J., Park, K., 2008. Oxidative stress and apoptosis induced by titanium dioxide nanoparticles in cultured BEAS-2B cells. Toxicol. Lett. 180 (3), 222–229. https://doi.org/10.1016/j.toxlet.2008.06.869.

Petkovic, J., Zegura, B., Stevanovic, M., Drnovsek, N., Uskokovic, D., Novak, S., Filipic, M., 2011. DNA damage and alterations in expression of DNA damage responsive genes induced by TiO_2 nanoparticles in human hepatoma HepG2 cells. Nanotoxicology 5, 341–353. https://doi.org/10.3109/17435390.2010.507316.

Popescu, T., Lupu, A.R., Raditoiu, V., Purcar, V., Teodorescu, V.S., 2015. On the photocatalytic reduction of MTT tetrazolium salt on the surface of TiO_2 nanoparticles: formazan production kinetics and mechanism. J. Colloid Interface Sci. 457, 108–120. https://doi.org/10.1016/j.jcis.2015.07.005.

Prasad, R.Y., Wallace, K., Daniel, K.M., Tennant, A.H., Zucker, R.M., Strickland, J., Dreher, K., Klingerman, A.,.D., Blackman, C.F., De Marini, D.M., 2013. Effect of treatment media on the agglomeration of titanium dioxide nanoparticles: impact on genotoxicity, cellular interaction, and cell cycle. ACS Nano 7, 1929–1942. https://doi.org/10.1021/nn302280n.

Proquin, H., Rodriguez-Ibarra, C., Moonen, C.G.J., Urrutia Ortega, I.M., Briede, J.J., de Kok, T.M., van Loveren, H., Chirino, Y.I., 2017. Titanium dioxide food additive (E171) induces ROS formation and genotoxicity: contribution of micro and nano-sized fractions. Mutagenesis 32, 139–149. https://doi.org/10.1093/mutage/gew051.

Reeves, J.F., Davies, S.J., Dodd, N.J.F., Jha, A.N., 2008. Hydroxyl radicals (●OH) are associated with titanium dioxide (TiO_2) nanoparticle-induced cytotoxicity and oxidative DNA damage in fish cells. Mutat. Res. 640 (1–2), 113–122. https://doi.org/10.1016/j.mrfmmm.2007.12.010. Epub 2007 Dec 31.

Sayes, C.M., Wahi, R., Kurian, P.A., Liu, Y., West, J.L., Ausman, K.D., Warheit, D.B., Colvin, V.L., 2006. Correlating nanoscale titania structure with toxicity: a cytotoxicity and inflammatory response study with human dermal fibroblast and human lung epithelial cells. Toxicol. Sci. 92, 174–185. https://doi.org/10.1093/toxsci/kfj197.

Schilirò, T., Bonetta, S., Alessandria, L., Gianotti, V., Carraro, E., Gilli, G., 2015. PM10 in a background urban site: chemical characteristics and biological effects. Environ. Toxicol. Pharmacol. 39 (2), 833–844. https://doi.org/10.1016/j.etap.2015.02.008.

Sha, B., Gao, W., Cui, W., Wang, L., Xu, F., 2015. The potential health challenges of TiO_2 nanomaterials. J. Appl. Toxicol. 35, 1086–1101. https://doi.org/10.1002/jat.3193.

Shi, H., Magaye, R., Castranova, V., Zhao, J., 2013. Titanium dioxide nanoparticles: a review of current toxicological data. Part. Fibre Toxicol. 10, 15. https://doi.org/10.1186/1743-8977-10-15.

Shi, Y., Wang, F., He, J., Yadav, S., Wang, H., 2010. Titanium dioxide nanoparticles cause apoptosis in BEAS-2B cells through caspase 8/t-Bid-independent mitochondrial pathway. Toxicol. Lett. 196, 21–27. https://doi.org/10.1016/j.toxlet.2010.03.014.

Tice, R.R., Agurell, E., Anderson, D., Burlison, B., Hartmann, A., Kobayashi, H., Miyamae, Y., Rojas, E., Ryu, J.C., Sasakim, Y.F., 2000. Single cell gel/Comet assay: guidelines

for in vitro and in vivo genetic toxicology testing. Environ. Mol. Mutagen. 35, 206–221 https://doi.org/10.1002/(SICI)1098-2280(2000)35:3 < 206::AID-EM8 > 3.0.CO;2-J.

Tomankova, K., Horakova, J., Harvanova, M., Malina, L., Soukupova, J., Hradilova, S., Kejlova, K., Malohlava, J., Licman, L., Dvorakova, M., Jirova, D., Kolarova, H., 2015. Cytotoxicity, cell uptake and microscopic analysis of titanium dioxide and silver nanoparticles in vitro. Food Chem. Toxicol. 82, 106–115. https://doi.org/10.1016/j.fct.2015.03.027.

Tompsett, G.A., Bowmaker, G.A., Cooney, R.P., Metson, J.B., Rodgers, K.A., Seakins, J.M., 1995. The Raman spectrum of brookite, TiO_2 (Pbca, Z = 8). J. Raman Spectrosc. 26, 57–62. https://doi.org/10.1002/jrs.1250260110.

Uboldi, C., Urban, P., Gilliland, D., Bajak, E., Valsami-Jones, E., Ponti, J., Rossi, F., 2016. Role of the crystalline form of titanium dioxide nanoparticles: rutile, and not anatase, induces toxic effects in Balb/3T3 mouse fibroblasts. Toxicol. Vitro 31, 137–145. https://doi.org/10.1016/j.tiv.2015.11.005.

Ursini, C.L., Cavallo, D., Fresegna, A.M., Ciervo, A., Maiello, R., Tassone, P., Buresti, G., Casciardi, S., Iavicoli, S., 2014. Evaluation of cytotoxic, genotoxic and inflammatory response in human alveolar and bronchial epithelial cells exposed to titanium dioxide nanoparticles. J. Appl. Toxicol. 34, 1209–1219. https://doi.org/10.1002/jat.3038.

Valant, J., Iavicoli, I., Drobne, D., 2012. The importance of a validated standard methodology to define in vitro toxicity of nano- TiO_2. Protoplasma 9, 493–502. https://doi.org/10.1007/s00709-011-0320-3.

Vevers, W.F., Jha, A.N., 2008. Genotoxic and cytotoxic potential of titanium dioxide (TiO_2) nanoparticles on fish cells in vitro. Ecotoxicology 17 (5), 410–420. https://doi.org/10.1007/s10646-008-0226-9. Epub 2008 May 20.

Wang, W., Gu, B., Liang, L., Hamilton, W.A., Wesolowski, D.J., 2004. Synthesis of rutile (α- TiO_2) nanocrystals with controlled size and shape by low-temperature hydrolysis: effects of solvent composition. J. Phys. Chem. B 108, 14789–14792. https://doi.org/10.1021/jp0470952.

Warheit, D.B., Donner, E.M., 2015. Risk assessment strategies for nanoscale and fine-sized titanium dioxide particles: recognizing hazard and exposure issues. Food Chem. Toxicol. 85, 138–147. https://doi.org/10.1016/j.fct.2015.07.001.

Weir, A., Westerhoff, P., Fabricius, L., Von Goetz, N., 2012. Titanium dioxide nanoparticles in food and personal care products. Environ. Sci. Technol. 46 (4), 2242–2250. https://doi.org/10.1021/es204168d.

Weyermann, J., Lochmann, D., Zimmer, A., 2005. A practical note on the use of cytotoxicity assays. Int. J. Pharm. 288, 369–376. https://doi.org/10.1016/j.ijpharm.2004.09.018.

Wilhelmi, V., Fischer, U., Van Berlo, D., Schulze-Osthoff, K., Schins, R.P.F., Albrecht, C., 2012. Evaluation of apoptosis induced by nanoparticles and fine particles in RAW 264.7 macrophages: facts and artefacts. Toxicol. Vitro 26, 323–334. https://doi.org/10.1016/j.tiv.2011.12.006.

Xu, J., Futakuchi, M., Iigo, M., Fukamachi, K., Alexander, D.B., Shimizu, H., Sakai, Y., Tamano, S., Furukawa, F., Uchino, T., Tokunaga, H., Nishimura, T., Hirose, A., Kanno, J., Tsuda, H., 2010. Involvement of macrophage inflammatory protein 1a (MIP1a) in promotion of rat lung and mammary carcinogenic activity of nanoscale titanium dioxide particles administered by intra-pulmonary spraying. Carcinogenesis 31, 5927–5935. https://doi.org/10.1093/carcin/bgq029.

Xue, C., Wu, J., Lan, F., Liu, W., Yang, X., Zeng, F., Xu, H., 2010. Nano titanium dioxide induces the generation of ROS and potential damage in HaCaT cells under UVA irradiation. J. Nanosci. Nanotechnol. 10, 8500–8507. https://doi.org/10.1166/jnn.2010.2682.

Zhang, J., Wang, J., Zhao, Z., Yu, T., Feng, J., Yuan, Y., Tang, Z., Liu, Y., Li, Z., Zou, Z., 2012. Reconstruction of the (001) surface of TiO_2 nanosheets induced by the fluorine-surfactant removal process under UV-irradiation for dye-sensitized solar cells. Phys. Chem. Chem. Phys. 14 (14), 4763–4769. https://doi.org/10.1039/c2cp24039d.